ECCOMAS Congress 2016
VII European Congress on Computational Methods in Applied Sciences and Engineering
M. Papadrakakis, V. Papadopoulos, G. Stefanou, V. Plevris (eds.)
Crete Island, Greece, 5–10 June 2016

NONLINEAR COMPOSITE VOXELS AND FFT-BASED HOMOGENIZATION

Matthias Kabel[1], **Andreas Fink**[1], **Felix Ospald**[2], **and Matti Schneider**[1]

[1]Department of Flow and Material Simulation
Fraunhofer ITWM
e-mail: {matthias.kabel,andreas.fink,matti.schneider}@itwm.fraunhofer.de

[2] Faculty of Mathematics
Chemnitz University of Technology
e-mail: felix.ospald@mathematik.tu-chemnitz.de

Keywords: Composite materials, Homogenization, Lippmann-Schwinger equation, FFT.

Abstract. *The FFT-based homogenization method of Moulinec-Suquet [14] has reached a degree of sophistication and maturity, where it can be applied to microstructures of industrial size and realistic scope. However, for non-linear or load-path-dependent problems the method reaches its limits, in particular if variations of the geometry are considered or the determination of the full material law on the macro-scale is required.*

Time and memory considerations are primarily responsible for these limitations. This work focuses on the composite voxel technique, where sub-voxels are merged into bigger voxels to which an effective material law based on laminates is assigned. Due to the down-sampled grid, both the memory requirements and the computational effort are severely reduced, while retaining the original accuracy. We discuss the extensions of linear elastic ideas [6, 9] to incremental problems at small strains. In contrast to conventional model order reduction methods, our approach does neither rely upon a "offline phase" nor on preselected "modes". We demonstrate our ideas with several numerical experiments, comparing to full-resolution computations heavily relying upon our MPI-parallel implementation FeelMath [1].

1 Introduction

In spite of the superior computational speed of FFT-based homogenization [13], direct nonlinear elastic computations [14, 11, 3, 8] on state-of-the-art CT images consisting of appr. 8000^3 voxels [2] cannot be considered as currently technically feasible. Therefore, the size of the structure has to be limited to a reasonable value by algorithmic improvements, such as the composite voxel technique [6, 9, 15].

In this paper, we first extend the composite voxel technique to physically nonlinear problems by affine linear approximation of the material laws in Section 2. Then, in Section 3 we apply the laminate and the Voigt mixing rule to a coarsely resolved long fiber reinforced plastic (LFT) microstructure (Fig. 2), compare the effective behavior to full resolution results and asses the possible speedup for linear and nonlinear simulations. Finally, in in Section 4 this algorithmic speedup is compared to the speedup due to an MPI parallelization

2 Composite voxels

The numerical execution of the so-called basic scheme of FFT-based homogenization [13] requires the evaluation of the stress tensor $\sigma(\epsilon, \epsilon_{\text{old}}, \ldots)$ in every voxel of the unit cell. If one is working directly on a CT image or, more generally, a voxelized geometry where every voxel is occupied by precisely one phase, the corresponding material law is applied. However, sometimes CT images are too large, or results are needed quickly, so that working on a cruder resolution seems inevitable. Then, the question arises how voxels containing more than one phase, so-called composite voxels, should be treated. In a preliminary work [9] that covered linearized elasticity the accuracy of various mixing rules were compared. In the work at hand we will concentrate on the Voigt and the laminate mixing rules.

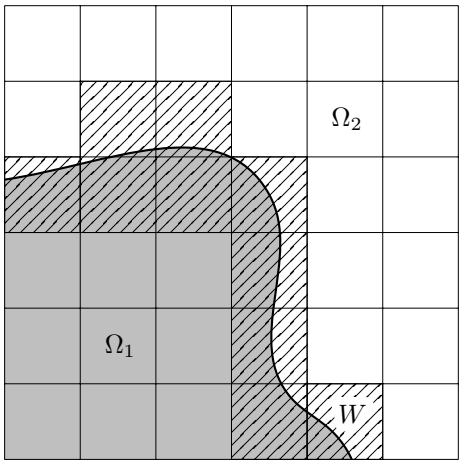

Figure 1: Voxelized geometry with composite voxels.

Before we go to the nonlinear case, we first recall these mixing rules. The Voigt mixing rule for a composite voxel W (see Fig. 1) reads $\mathbb{C}_W^{\text{Voigt}} = \langle \mathbb{C} \rangle$, where $\langle \cdot \rangle$ denotes the spatial average according. The Voigt average $\mathbb{C}_W^{\text{Voigt}}$ constitutes an upper bound on the effective elastic tensor. For a composite voxel W containing precisely two constituents the laminate mixing rule assumes that the interface between the phases is approximately linear with normal vector n. Inspired by the formula for a general laminate, cf. Milton [12, Section 9.5], the elastic tensor of the laminate mixing rule is obtained by solving the system

$$\left(\mathbb{P} + \lambda(\mathbb{C}_W^{\text{laminate}} - \lambda\,\mathrm{Id})^{-1}\right)^{-1} = \left\langle \left(\mathbb{P} + \lambda(\mathbb{C} - \lambda\,\mathrm{Id})^{-1}\right)^{-1} \right\rangle,$$

where the four-tensor

$$\mathbb{P}_{ijlm} = \frac{1}{2}\left(n_i\delta_{jl}n_m + n_i\delta_{jm}n_l + n_j\delta_{il}n_m + n_j\delta_{im}n_l\right) - n_in_jn_ln_m$$

encodes the interface direction n and $\lambda > 0$ is chosen sufficiently large. More precisely, λ should be larger than the largest eigenvalue of the stiffness matrices $\mathbb{C}(x)$ for all x.

We extend these mixing rules to the physical nonlinear case in three steps

1. Linearization: In every loading step the (nonlinear) material laws are linearized at the deformed state ϵ^n of the composite voxel

$$\mathbb{C}(x) = \frac{\partial \sigma}{\partial \epsilon}(x, \epsilon^n, \epsilon^{n-1}, \ldots)$$

2. Mixing: The effective linearized stiffness $\mathbb{C}_W$ is calculated according to the consistent mixing rules for the linear elastic case. The nonlinear behavior of the composite voxel is approximated by the affine linear function

$$\sigma(\epsilon^{n+1}, \epsilon^n, \ldots) = \sigma^n + \mathbb{C}_W : (\epsilon^{n+1} - \epsilon^n)$$

3. Internal variables: The internal variables of the constituents are updated due to the deformation ϵ^{n+1} of the composite voxel.

3 Long Fiber Reinforced Thermoplastic (LFT)

Long-fiber reinforced thermoplastics (LFT) bridges the price-to-performance gap between short fiber thermoplastic (SFT) materials and continuous fiber composite materials while still being processable via efficient injection or compression molding methods [18, 16, 7]. The investigated material, produced by compression molding, features an extremely high maximum fiber length of approx. 50 mm and a corresponding aspect ratio of approximately 3000. To incorporate the complete fiber length spectrum and thereby conserve the scale separation, the size of the representative volume elements of the LFT structure would be extremely large and outside the limits of computational resources, if equal edge lengths of the RVE would be considered, as pointed out in the following: Glass fibers have a diameter ranging between 5 μm and 24 μm. This enforces a minimal resolution of 5 μm. Considering a value of 50 mm for the maximum fiber length, the RVE needs to be discretized with 10000^3 voxels. To limit the size of the structure to a reasonable value, the maximum fiber length is therefore exclusively implemented in flow direction (the longest RVE edge), whereas the transverse directions are cropped, resulting in differing edge lengths, see Figure 2.

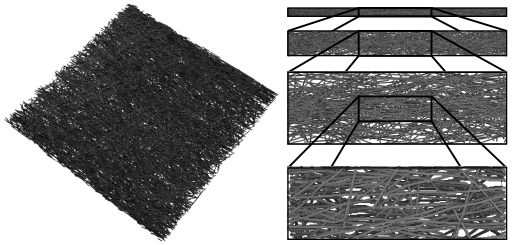

Figure 2: Virtually generated LFT microstructure [5] (left). Part of the LFT microstructure used for simulations (right). Sample size: $40 \times 1.5 \times 0.134$ mm^3. Discretization: $8000 \times 300 \times 27$ voxels.

3.1 Material parameters

The investigated LFT material consists of a polypropylene matrix (DOW® C711-70RNA) and 30 wt% glass fibers (TufRov® 4575). As specified by the manufacturer, in the linear elastic regime the glass fibers are characterized by a Young's modulus of $E_{glass} = 72$ GPa and Poisson's ratio of $\nu_{glass} = 0.2$, whereas for the polypropylene (PP) matrix we have a Young's modulus $E_{PP} = 1.25$ GPa and a Poisson's ratio of $\nu_{PP} = 0.35$.

For uniaxial tension of polypropylene Fig. 3 contains the measured stress-strain curve as determined by Fliegener [4]. The behavior is linear initially, followed by a plastic phase, roughly up to 5% strain. For higher strains, a strain softening effect is observed, which is commonly attributed to fracture or damage effects. However, as the regime of 5% strain and higher usually demands a description by large deformations, we neglect this strain-softening effect, and rely upon an incremental elastic-plastic material law at small strains governed by a J_2-flow theory with isotropic hardening. To approximate the nonlinear curve of Fig. 3 we rely upon a piecewise linear hardening curve. The fitting is reasonably accurate up to a relative strain of 5%.

ϵ^p_{eq} [%]	0	1.33697	2.37197	4.08397
σ_{eq} [MPa]	12	16	18	19

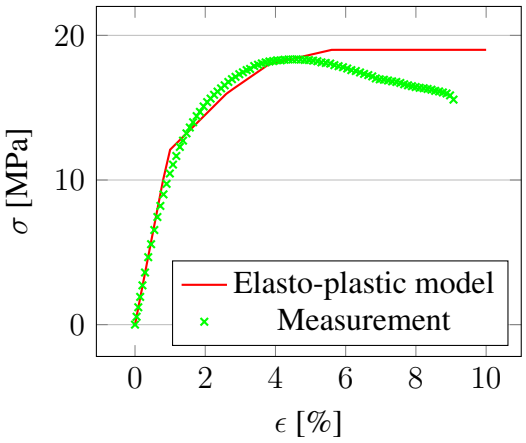

Figure 3: Calibrated hardening parameters for PP (top). Tensile tests of PP and calibrated elasto-plastic model [4] (bottom).

3.2 Numerical results

All simulation were performed on the part of the virtual microstructure shown in Fig. 2 (right) consisting of $8000 \times 300 \times 27$ voxels, which is discretized on a staggered grid [17]. Therefore, the resulting discretized problems have 194.4 million (displacement) degrees of freedom. By downsampling the geometry by a factor of 2 resp. 4 we obtain two alternative discretizations with composite voxels, see Fig. 4. Technical details concerning the downsampling procedure with composite voxels can be found in [9].

In the linear elastic case 6 loading cases were performed which allow to calculate the effective stiffness $\mathbb{C}_{\text{eff}}$ of the LFT. To compare the effective stiffnesses for different numerical methods, the direction-dependent Young's moduli in the fiber plane are evaluated, see Fig. 5. The direction-dependent Young's

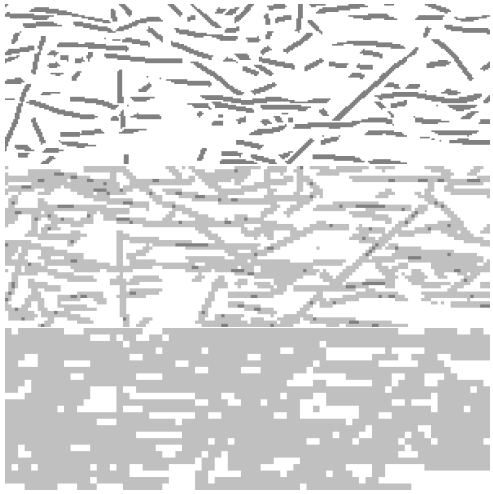

Figure 4: Slice of the LFT microstructure at full resolution (top), half resolution (middle) and quarter resolution (bottom) which contain PP (white), Glass (dark gray) and composite voxels (light gray)

modulus is defined by

$$\frac{1}{E(d)} = (d \otimes d) \cdot \mathbb{C}_{\text{eff}}^{-1} : (d \otimes d)$$

with

$$d = \begin{pmatrix} \cos(\alpha) \\ \sin(\alpha) \\ 0 \end{pmatrix}$$

The relative error of the numerical solutions using composite voxels on downsampled geometries exhibits the following behavior

- Laminate mixing: The effective stiffness is underestimated. At both half and quarter resolution the relative error has its maximum at appr. $40°$. The relative error stays below 7% and 24% respectively. Orthogonal to the main fiber direction the relative error is below 1% for both resolutions. In main fiber direction the relative error is appr. 4% and 17% respectively

- Voigt mixing: The effective stiffness is overestimated. At both half and quarter resolution the relative error has its maximum at appr. $10°$. The relative error stays below 8% and 20% respectively. Orthogonal to the main fiber direction the relative error is below 3% and 8% respectively. In main fiber direction the relative error is appr. 8% and 19% respectively

In light of to the fluctuations of the three measurements in $0°$ and $90°$-direction [4] it is reasonable to perform linear elastic simulations on the half resolution even if the original geometry resolves the fibers only with 3 voxels over the diameter.

Due to the results for the linear elastic case we decided to perform the nonlinear simulations only at full and half resolutions. In Fig. 5 we compare the results of simulated uniaxial tensile tests with measurements and investigate the evolution of the relative error for increasing loading. At the beginning both mixing rules start with a relative error slightly below 20%. While the relative error for the Voigt mixing rapidly increases and reaches 37% at the end of the loading, the error decreases monotonously for laminate mixing. Taking into account the variance of the experimental results for the uniaxial tensile tests in main fiber direction, the error due to downsampling by a factor of 2 is acceptable if laminate composite voxels are used.

3.3 Computational effort

After assessing the quality of the numerical solution we study the speedup on for downsampled geometries with composite voxels. For the linear elastic case we apply the conjugate gradient method (CG) to accelerate the convergence speed of FFT-based homogenization [19]. Since composite voxels lead to a smoothing of the material contrast at the interfaces, one could expect less iterations for the problems on the downsampled geometries. As observed by Kabel et al. [9] this is not the case, see Tab. 1. For linear elastic problems composite voxels do not influence the convergence speed. According to Tab. 3 using half resolution with composite voxels reduces

Resolution	Mixing rule	# Iterations
Full	-	1049
Half	Laminate	1007
	Voigt	1054
Quarter	Laminate	954
	Voigt	1076

Table 1: Number of iterations for 6 loadcases.

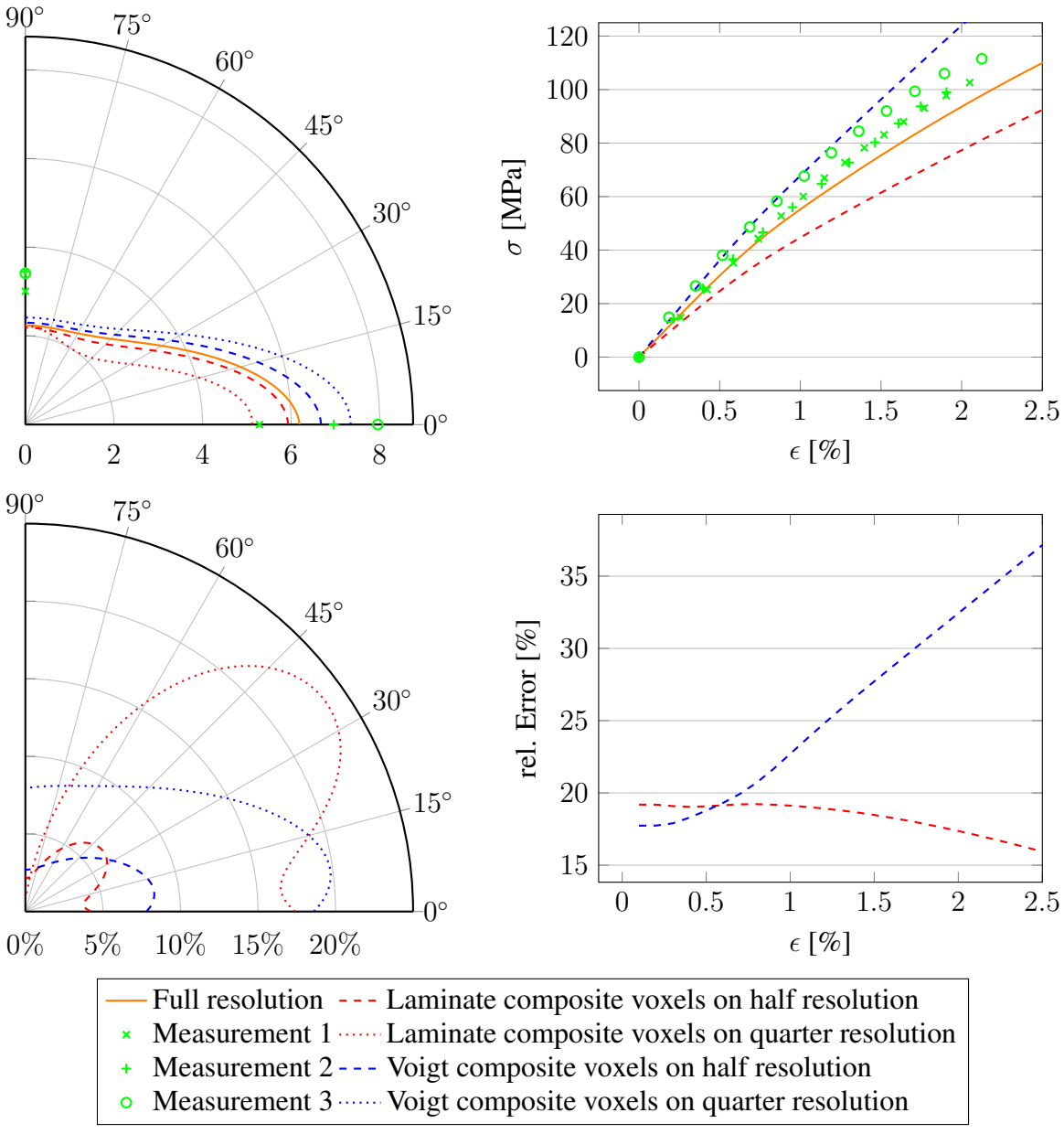

Figure 5: Young's modulus body [GPa] in x-y-plane (top left) and relative error (bottom left). Simulated tensile test in main fiber direction (top right) and relative error of the results with using composite voxels (bottom right).

Resolution	Laminate			Voigt		
	Total [s]	FFT [s]	Material [s]	Total [s]	FFT [s]	Material [s]
Full	8423	6706	1643	8423	6706	1643
Half	4691	2316	2316	3540	2421	1080
Quarter	3511	1034	2433	1974	1165	787
Full	59452	17593	38519	59452	17593	38519
Half	8416	682	7409	6493	699	5568

Table 3: Computational effort of 10 cores for composite voxels on half (24.3 million DOFs) and quarter (3.0375 million DOFs) resolution in comparison to the effort of full-resolution (194.4 million DOFs) computations. Linear elasticity (top). Von Mises plasticity (bottom)

the computational time by 45% for laminate mixing and 58% for Voigt mixing compared to full resolution simulations.

Since the volume fraction of the composite voxels increases dramatically at quarter resolution, see Tab. 2, and the evaluation of the stress response for composite voxels is computationally more expensive than evaluating linear elastic material laws, no further significant speedup can be obtained on coarser geometries. To be more precise, using quarter resolution with laminate composite voxels reduces the runtime by 58% and is approximately as fast as Voigt mixing at half resolution. Quarter resolution with Voigt mixing reduces the runtime by 76%.

Resolution	PP	Glass	Composite
Full	86.77	13.23	0.00
Half	57.78	2.61	39.61
Quarter	27.51	0.00	72.49

Table 2: Volume fractions [vol%] for the LFT microstructure

The physically nonlinear case we use the basic scheme developed by Moulinec-Suquet [14]. In contrast to the linear case, the number of iterations needed for convergence is significantly reduced by using composite voxels, see Fig. 6. This effect is due to the linearization of the composite voxels. As a side effect also the repeated application of the material law in the composite voxels is less expensive than applying the original nonlinear material law, see Tab. 3. At half resolution using laminate mixing decreases the total runtime by 85 % and using Voigt mixing even decreases it by 90 %.

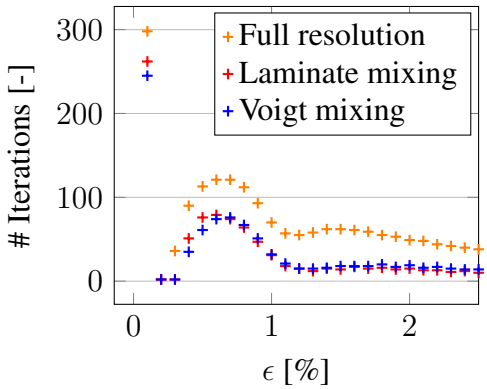

Figure 6: Number of iterations needed for convergence for the tensile tests in main fiber direction at full and half resolution.

4 Parallel efficiency

If highly accurate results are needed it is possible to accelerate the simulations by parallelization of the algorithm. In this section we will study the possible speedup for an MPI parallelization of the basic scheme. Since all operations of the basic scheme except for the fast Fourier transform (FFT) are local operations, the parallel efficiency depends crucially on the implementation of FFT. For computing the discrete Fourier transform we are using the C

Cores	Total [s]	Efficiency [%]	FFT [s]	Efficiency [%]	Material [s]	Efficiency [%]
10	8423	100	6706	100	1643	100
20	4243	99	3332	101	871	94
40	2653	79	2134	79	494	83
80	1485	71	1214	69	242	85
160	876	60	727	58	121	84
320	584	45	455	46	65	78
10	59451	100	17593	100	38519	100
20	32332	92	12351	71	18408	105
40	14785	100	4876	90	9129	105
80	7481	99	4609	48	4609	104
160	3931	95	2307	48	2307	104
320	2280	81	1124	49	1124	107

Table 4: Parallel efficiency for full-resolution (194.4 million DOFs) simulations. Linear elasticity (top). Von Mises plasticity (bottom).

(subroutine) library FFTW[1].

All simulations have been performed on the Beehive cluster at Fraunhofer ITWM, which consists of 192 nodes (Dell Power Edge M620) each having a dual Intel Xeon E5-2670 (”Sandy Bridge”) processor, i.e 16 CPU Cores per node. The nodes are connected by FDR Infiniband.

4.1 Strong scaling

In the linear elastic case FFT runtime dominates the numerical effort, see Tab. 4 and Fig. 7. Therefore, also the parallel effiency of the FFT-based scheme almost coincides with the parallel efficiency of FFT. In comparison to composite voxels the runtime on 2 nodes is similar to solving the problem at half resolution on 1 node and the runtime on 4 nodes is similar to that on 1 node at quarter resolution.

In the physically nonlinear case the material law dominates the numerical effort. Since the parallel efficiency of applying the material law is perfect in our example, the total parallel efficiency is greater than 82 % for up to 32 nodes and 320 MPI processes, see Tab. 4. Nonetheless using the composite voxel technique with half resolution, 8 times more nodes are required to have comparable runtimes.

5 Conclusion

Previous studies on the composite voxel technique always assumed highly resolved objects. In many application it is currently not possible to obtain CT-images (or virtually generated microstructures) that are representative and additionally resolve all objects well. For LFT it is a rule of thumb to make CT-Images with a resolution that correspond to 3 - 4 voxels over the diameter of the fibers. Therefore, at first glance the application of the composite voxels technique to LFT microstructures seemed to be questionable. Nonetheless it tuned out, that for both linear and nonlinear material modelling of LFT, simulations at half resolution with laminate composite voxels give reasonable results from an engineering point of view and lead to a significant speedup.

[1] www.fftw.org

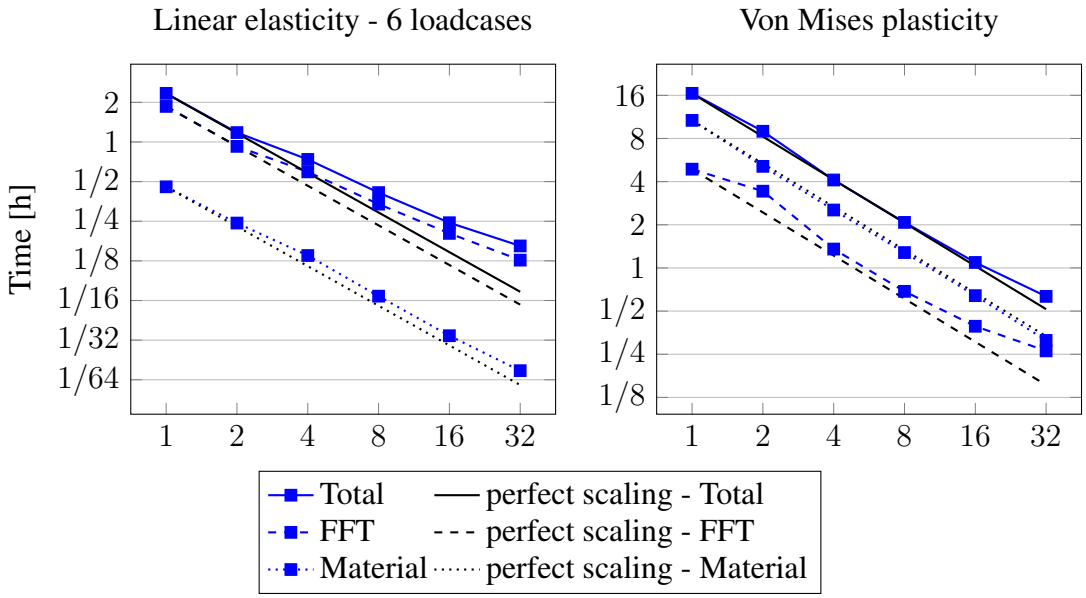

Figure 7: Strong scaling for 10 MPI processes per node.

Concerning the relative error of the effective linear elastic behaviour, the laminate mixing rule consistently outperforms the Voigt mixing rule at half resolution but fails at quarter resolution when the interface directions calculated in the downsampling process are no longer meaningful (the complete cross section of a fiber can be contained in a composite voxel). More strikingly, the relative error of the effective stress-strain curve considered as a function of the applied load decreases when using composite voxels with laminate mixing whereas it grows linearly for Voigt mixing. Thus, working on a coarser resolution for physically nonlinear problems is only acceptable in combination with laminate mixing.

To further increase the precision of laminate mixing in the physically nonlinear case we will consider direct laminate mixing of nonlinear material laws in a future work [10].

Acknowledgements

While writing this article, Felix Ospald received financial support from the German Research Foundation (DFG), Federal Cluster of Excellence EXC 1075 “MERGE Technologies for Multifunctional Lightweight Structures”.

REFERENCES

[1] FeelMath. Fraunhofer ITWM `http://www.itwm.fraunhofer.de/feelmath`. Accessed: 2015-11-20.

[2] High-Resolution Computed Tomography flyer. NEXT ENERGY EWE-Forschungszentrum für Energietechnologien e.V. Accessed 12.02.2016, `http://www.next-energy.de/tl_files/pdf/NE_Flyer_CT_2014_EN.pdf`.

[3] P. Eisenlohr, M. Diehl, R.A. Lebensohn, and F. Roters. A spectral method solution to crystal elasto-viscoplasticity at finite strains. *International Journal of Plasticity*, 46(0):37–53, 2013.

[4] S. Fliegener. *Micromechanical finite element modeling of long fiber reinforced thermoplastics*. PhD thesis, Karlsruhe Institute of Technology (KIT), 2015.

[5] S. Fliegener, M. Luke, and P. Gumbsch. 3d microstructure modeling of long fiber reinforced thermoplastics. *Composites Science and Technology*, 104(0):136 – 145, 2014.

[6] L. Gélébart and F. Ouaki. Filtering material properties to improve fft-based methods for numerical homogenization. *J. Comput. Phys.*, 294(C):90–95, August 2015.

[7] Henning F, Ernst H, Brüssel R, Geiger O, Krause W. LFTs for automotive applications. *Reinforced Plastics*, 49:24–33, 2005.

[8] M. Kabel, T. Böhlke, and M. Schneider. Efficient fixed point and Newton-Krylov solvers for FFT-based homogenization of elasticity at large deformations. *Computational Mechanics*, 54(6):1497–1514, 2014.

[9] M. Kabel, D. Merkert, and M. Schneider. Use of composite voxels in FFT-based homogenization. *Computer Methods in Applied Mechanics and Engineering*, 294(0):168–188, 2015.

[10] M. Kabel and M. Schneider. Physically nonlinear composite voxel. In preparation.

[11] N. Lahellec, J.C. Michel, H. Moulinec, and P. Suquet. Analysis of inhomogeneous materials at large strains using fast fourier transforms. In Christian Miehe, editor, *IUTAM Symposium on Computational Mechanics of Solid Materials at Large Strains*, volume 108 of *Solid Mechanics and Its Applications*, pages 247–258. Springer Netherlands, 2003.

[12] G. W. Milton. *The Theory of Composites*. Cambridge University Press, 2002. Cambridge Books Online.

[13] H. Moulinec and P. Suquet. A fast numerical method for computing the linear and nonlinear mechanical properties of composites. *Comptes rendus de l'Académie des sciences. Série II, Mécanique, physique, chimie, astronomie*, 318(11):1417–1423, 1994.

[14] H. Moulinec and P. Suquet. A numerical method for computing the overall response of nonlinear composites with complex microstructure. *Computer Methods in Applied Mechanics and Engineering*, 157(1-2):69–94, 1998.

[15] F. Ospald, M. Schneider, and M. Kabel. Hyperelastic laminates, composite voxels and FFT-based homogenization at finite strains. *Computer Methods in Applied Mechanics and Engineering*, submitted.

[16] C.W. Peterson, G. Ehnert, R. Liebold, and R. Kühfusz. Compression molding. In D.B. Miracle and S.L. Donaldson, editors, *Composites*, volume 21 of *ASM Handbook*, pages 516–535. Springer Netherlands, 2001.

[17] M. Schneider, F. Ospald, and M. Kabel. Computational homogenization of elasticity on a staggered grid. *International Journal for Numerical Methods in Engineering*, 105(9):693–720, 2016.

[18] R.H. Todd, D.K. Allen, and L. Alting. *Manufacturing Processes Reference Guide*. Industrial Press, 1994.

[19] J. Zeman, J. Vondřejc, J. Novák, and I. Marek. Accelerating a FFT-based solver for numerical homogenization of periodic media by conjugate gradients. *Journal of Computational Physics*, 229(21):8065 – 8071, 2010.